Synthesis and characterization of an antibacterial powder based on the covalent bonding of aminosilane-stabilized silver nanoparticles to a colloidal silica

I. E. dell'Erba, A. Y. Mansilla, C. E. Hoppe & R. J. J. Williams

Journal of Materials Science
Full Set - Includes `Journal of Materials Science Letters'

ISSN 0022-2461

J Mater Sci
DOI 10.1007/s10853-015-9700-y

Springer

Your article is protected by copyright and all rights are held exclusively by Springer Science +Business Media New York. This e-offprint is for personal use only and shall not be self-archived in electronic repositories. If you wish to self-archive your article, please use the accepted manuscript version for posting on your own website. You may further deposit the accepted manuscript version in any repository, provided it is only made publicly available 12 months after official publication or later and provided acknowledgement is given to the original source of publication and a link is inserted to the published article on Springer's website. The link must be accompanied by the following text: "The final publication is available at link.springer.com".

Author's personal copy

J Mater Sci
DOI 10.1007/s10853-015-9700-y

Synthesis and characterization of an antibacterial powder based on the covalent bonding of aminosilane-stabilized silver nanoparticles to a colloidal silica

I. E. dell'Erba[1] · A. Y. Mansilla[2] · C. E. Hoppe[1] · R. J. J. Williams[1]

Received: 4 November 2015 / Accepted: 22 December 2015
© Springer Science+Business Media New York 2015

Abstract Stable dispersions of silver nanoparticles (Ag NPs) were synthesized employing glycerol as both a solvent and reducing agent, and 3-aminopropyl trimethoxysilane (APTMS) as a stabilizer. Average sizes varied between 13 and 55 nm, depending on the molar ratio of APTMS/Ag. Terminal alkoxysilanes reacted with OH groups of glycerol leading to the covalent bonding of glycerol moieties to the chain ends of the stabilizer. This produced extremely stable colloidal dispersions from which NPs could not be extracted with solvents immiscible with glycerol (as THF). Ag NPs were covalently bonded to the surface of a colloidal silica by hydrolysis/condensation of terminal Si–O–C bonds of the stabilizer with superficial SiOH bonds of silica. TEM images revealed the presence of individual NPs and small clusters of NPs attached to the silica surface. These clusters were presumably generated by intermolecular reactions among chain ends of the stabilizer producing Si–O–Si bonds. The antibacterial properties of the resulting powder were confirmed by conventional tests employing a culture of *Escherichia Coli*.

✉ I. E. dell'Erba
ideller@mdp.edu.ar

[1] Institute of Materials Science and Technology (INTEMA), University of Mar del Plata and National Research Council (CONICET), Av. J. B. Justo 4302, 7600 Mar del Plata, Argentina

[2] Biological Research Institute (IIB), University of Mar del Plata and National Research Council (CONICET), Funes 3250, CC 1245, 7600 Mar del Plata, Argentina

Introduction

The antibacterial properties of silver nanoparticles (Ag NPs) have been extensively discussed and reviewed [1–3], and they have found applications in clothing, medical devices, and food containers [4–6]. However, one concern about the use of free Ag NPs is their toxicity over living beings, including humans [7, 8]. Therefore, for practical applications as an antibacterial additive, it is convenient to produce the covalent bonding of Ag NPs to an adequate support. As colloidal silica is used as a filler and reinforcing agent for many polymeric formulations, it was our interest to investigate the possibility of producing the covalent bonding of Ag NPs to a commercial silica to provide the reinforced material with antibacterial properties. Aminosilanes are convenient linkers to produce the desired covalent bonding. The amino group which is present at one end of the linker coordinates with Ag atoms present at the surface of Ag NPs [9, 10]. The alkoxysilane groups present at the other end can be hydrolyzed and condensed with SiOH groups present at the silica surface, generating the desired covalent bonds.

The proposed strategy has been used in different ways in the past. One way was to synthesize an organically modified silica (Ormosil) by the co-condensation of an aminosilane with tetraethoxysilane (TEOS) in the presence of an Ag^+ salt and hydrazine as a reducing agent [11, 12]. Ormosils doped with Ag NPs were successfully obtained and their antimicrobial properties assessed. A second way was the aminosilane modification of a porous ceramic based on diatomite and clay [13]. The amino groups decorating the pores enabled to fix previously synthesized silver nanoparticles stabilized with polyvinylpyrrolidone (PVP) [13]. Presumably, the partial substitution of PVP segments by amino groups enabled to fix Ag NPs inside the pores. The resulting composite was employed as an antibacterial water filter.

Published online: 04 January 2016

Author's personal copy

A much simpler strategy was used in this study. Ag NPs sere synthesized in the presence of an aminosilane as a stabilizer, using glycerol as both a solvent and a reducing agent. The average size of the Ag NPs depended on the relative amount of the aminosilane used in the synthesis. Aminosilane-stabilized Ag NPs were covalently bonded to a commercial colloidal silica and the antibacterial properties of the resulting material were determined.

Materials and methods

Synthesis of Ag NPs

A typical reaction batch consisted in 1.5 g of anhydrous glycerol (Cicarelli, 99.5 %) and 75 mg of $AgNO_3$ (ACS reagent, purity >99 %, Sigma-Aldrich). After dissolution of the salt with stirring at 50 °C, the appropriate amount of 3-aminopropyl trimethoxysilane (APTMS, purity >97 %, Fluka) was added and the reaction was conducted during 1 h. Then, stirring was stopped and the resulting colloidal solution cooled to room temperature. Three molar ratios were employed: APTMS/Ag = 2, 4 and 8. Resulting Ag NPs will be denoted as NP2, NP4, and NP8, respectively.

It is important to mention that formation of silver nanoparticles was not achieved when $AgNO_3$ was dissolved in water before adding it to glycerol. As shown by Frattini et al. [9], the aminosilane acts both as a catalyst of the reduction, coordinating to Ag^+ cations, and as a stabilizer of the Ag NPs generated. The dissolution of the silver salt in water generates $Ag(H_2O)_n^+$ complexes that hinder the coordination of the aminosilane and prevent (or retard) the reduction with glycerol.

Covalent bonding of Ag NPs to the colloidal silica

Typically, 1.5 g of the colloidal dispersion of Ag NPs in glycerol was washed three times with tetrahydrofuran (THF, Cicarelli), a solvent that is not miscible with glycerol. Then 1 g of a commercial colloidal silica (Aerosil OX 50, Degussa, specific area of 50 m^2/g and around 6.10^{-6} mol OH/m^2) was added together with 5 ml of THF and 0.5 ml of aqueous NaOH 0.02 M, with strong stirring. After 24 h reaction, the slurry was washed with water and centrifuged at 6000 rpm for 5 min. This process was repeated several times until the supernatant became completely uncolored. The solid product was then dried at 110 °C for 2 h and ground.

Characterization techniques

The absorption spectra of diluted colloidal dispersions of Ag NPs in water were measured with an UV–visible spectrophotometer (1601 PC, Shimadzu), at room temperature. Fourier-transformed infrared (FTIR) spectra were obtained with a Genesis II-Mattson device in the DRIFTS mode. Powders were ground and mixed with spectroscopic-grade KBr, and 64 scans were averaged. XRD spectra were recorded with an XPert Pro PANalytical device, with the wavelength of Cu Kα (1.5406 Å). Liquid or solid samples were placed on a glass substrate. Transmission electron microscopy (TEM) was carried out using a Philips CM-12 device operated at an accelerating voltage of 100 kV. Samples were supported over a copper grid coated with formvar and a carbon film.

The contents of silver fixed on the nanoparticles were determined by inductively coupled plasma emission spectroscopy (ICP) at the Federal University of Rio Grande do Sul (UFRGS, Brazil). Samples of SiO_2-NP were treated with HNO_3 to dissolve Ag and analyzed in a Perkin Elmer Optima 7300 device.

Antibacterial properties

Cultures of *Escherichia Coli* were grown in Luria–Bertani medium (LB) in test tubes until they reached the log phase. One of these tubes was used as a control (Control [+]), another tube (Control [−]) was supplemented with 0.05 wt% ampicillin (a beta-lactam antibiotic), and the remaining tubes were supplemented with 1 wt% untreated commercial silica or with different amounts of NP4-SiO_2 (from 0.2 to 2 wt%). Tubes were kept at 37 °C with continuous shaking. Bacterial growth was determined by measuring optical density (OD) at 600 nm, after 3, 5, and 24 h.

Results and discussion

Characterization of Ag NPs

The colloidal dispersion of Ag NPs in glycerol was completely stable as corroborated for tubes stored for more than 1 year. No signs of precipitation or aggregation were observed and UV–visible spectra remained unmodified. Besides, Ag NPs were not extracted from the glycerol phase when using THF to remove side products. The explanation of the high stability of the colloidal dispersion and the insolubility of Ag NPs in THF relies on the expected reaction of Si–O–CH_3 groups with hydroxyl groups of glycerol:

$$Si{-}O{-}CH_3 + OH{-}C{-} \rightarrow Si{-}O{-}C{-} + CH_3OH.$$

The reaction of alkoxysilane groups with alcohols has been reported in the literature [14–16]. In the present case, this reaction replaces a fraction of terminal methoxysilane groups by glycerol moieties, a fact that explains both the

Author's personal copy

high stability of the colloidal dispersion in glycerol and the insolubility of Ag NPs in THF. The generated Si–O–C groups behave in a similar way as Si–O–CH_3 groups with respect to their hydrolysis and condensation with SiOH groups present at the silica surface. Therefore, the reaction of Si–O–CH_3 groups with glycerol does not affect the ulterior covalent bonding of Ag NPs to the silica surface.

Figures 1 and 2 show TEM images of Ag NPs and the corresponding particle size distributions.

The broad particle size distributions were approximately fitted with Gaussian curves. Average sizes were 55 nm for NP2, 23 nm for NP4, and 13 nm for NP8. The average diameters decreased with an increase in the aminosilane amount used in the synthesis, as previously reported and explained in the literature [10]. A significant fraction of very tiny particles was also observed in the TEM image of NP8. In fact, this sample contained a bimodal distribution of NPs but only the particles with larger sizes were considered to determine the average size.

In order to obtain UV–visible spectra, the colloidal dispersion of Ag NPs in glycerol was diluted with a high excess of water to reduce the intensity of the plasmon band to an appropriate value (dilution with glycerol was also performed leading to similar spectra).

Figure 3 shows the UV–visible spectra for Ag NPs synthesized with different APTMS/Ag molar ratios. For APTMS/Ag = 8, the maximum of the Ag plasmon band is

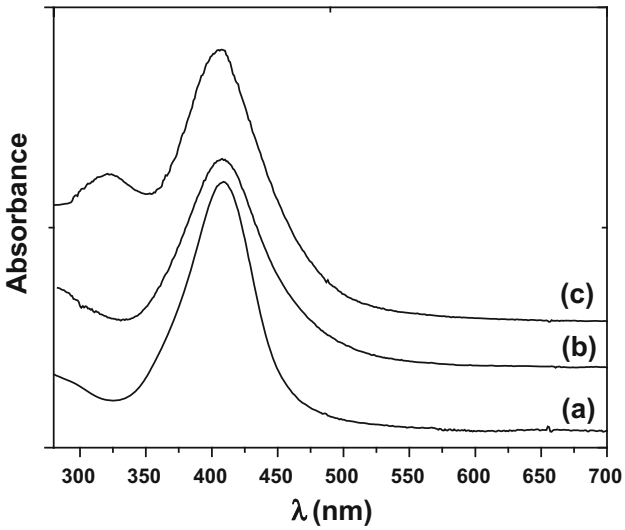

Fig. 3 UV-visible spectrum of the colloidal dispersion of Ag NPs synthesized with different APTMS/Ag molar ratios **a** APTMS/Ag = 2, **b** APTMS/Ag = 4, **c** APTMS/Ag = 8

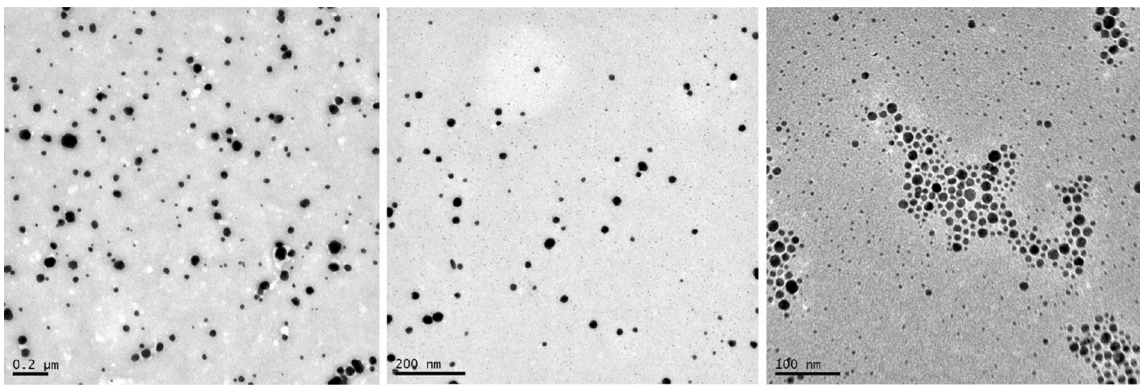

Fig. 1 TEM images of Ag NPs, from *left* to *right*: NP2, NP4, and NP8

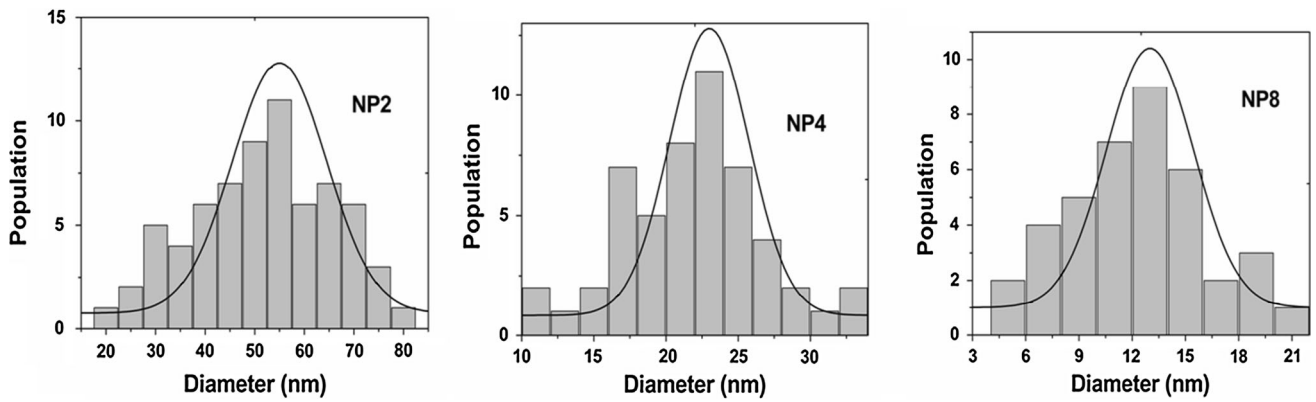

Fig. 2 Particle size distributions of NP2, NP4, and NP8

Author's personal copy

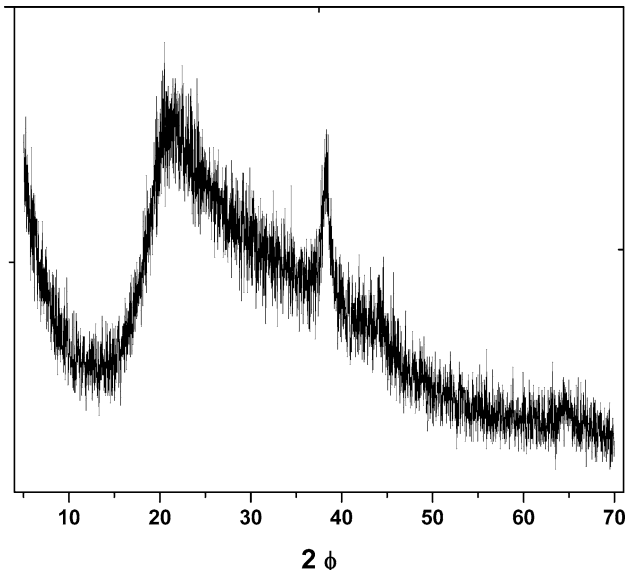

Fig. 4 XRD spectrum of the colloidal dispersion of Ag NPs in glycerol

located at 407 nm, with a width at half height of 74 nm. A smaller broad peak centered at 321 nm is assigned to the presence of Ag clusters or very small NPs that were found in TEM images (Fig. 1) [17]. For the other two molar ratios, only the peak of the Ag plasmon band was observed. The maximum is located at 408 nm for NP4 (69 nm width at half weight), and 410 nm for NP2 (56 nm width at half weight). Therefore, increasing the average size of the NPs produced a small shift of the maximum of the plasmon band to the red (from 407 to 410 nm), and reduced the width at half weight (from 74 to 56 nm). These trends agree with those reported in the literature [9].

The XRD spectrum of the colloidal dispersion of Ag NPs in glycerol is shown in Fig. 4. The diffraction peak at $2\phi = 38.2°$ corresponds to the (111) plane of face-centered cubic (fcc) crystalline silver [13]. Other characteristic peaks of crystalline silver were not observed due to the small concentration of Ag NPs in the colloidal dispersion.

Bonding of Ag NPs to colloidal silica

Figure 5 shows photographs of the colloidal dispersion of Ag NPs in glycerol, the commercial colloidal silica, and three samples of the colloidal silica powder decorated by Ag NPs. The covalent bonding of Ag NPs to the silica surface was proved by FTIR spectra using the characteristic peak of free SiOH groups at 3746 cm^{-1}. Figure 6 shows that this peak disappeared after reaction with the colloidal dispersion of Ag NPs, revealing the generation of covalent Si–O–Si bonds between the silica surface and the aminosilane stabilizers. This was also confirmed by a blank

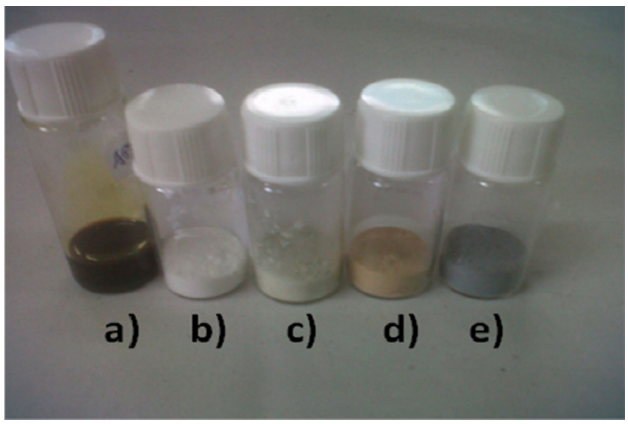

Fig. 5 **a** Colloidal dispersion of Ag NPs in glycerol, **b** commercial colloidal silica, **c** NP2-silica, **d** NP4-silica, **e** NP8-silica

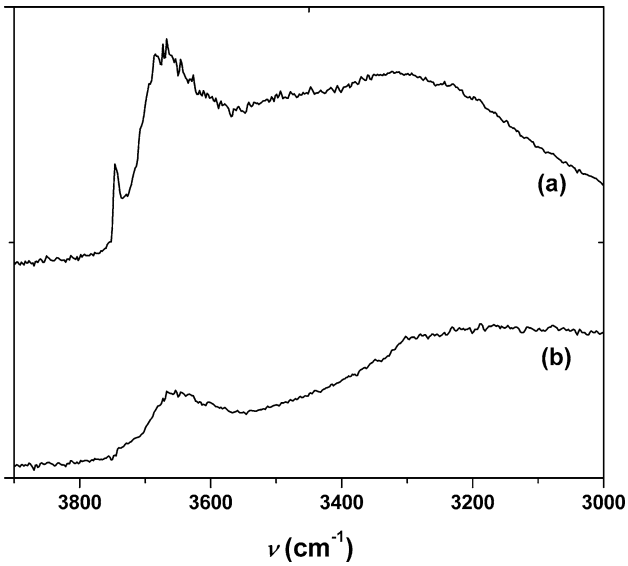

Fig. 6 FTIR spectra of **a** colloidal silica, **b** colloidal silica with covalently bonded NP4 silver nanoparticles

test carried out in the absence of Ag NPs that showed the persistence of the characteristic peak of free SiOH groups.

XRD spectra (Fig. 7) also proved that modification of silica surface with Ag NPs was successful. Characteristic diffraction peaks of crystalline fcc silver at 38.2°, 44.3°, and 64.7°, corresponding to the 111, 200, and 220 planes [13], respectively, are observed. The presence of three characteristic peaks with a significant intensity arises from the location of Ag NPs at the surface of the colloidal silica.

The average particle diameter can be estimated using Scherrer's equation [18, 19]:

$$d = k\lambda/(B\cos\phi).$$

Scherrer's constant is $k = 0.94$, valid for spherical crystals with cubic symmetry; $\lambda = 0.15406$ nm is the wavelength of the X-ray radiation, $\phi = 38.22°/2$ is Bragg's

Author's personal copy

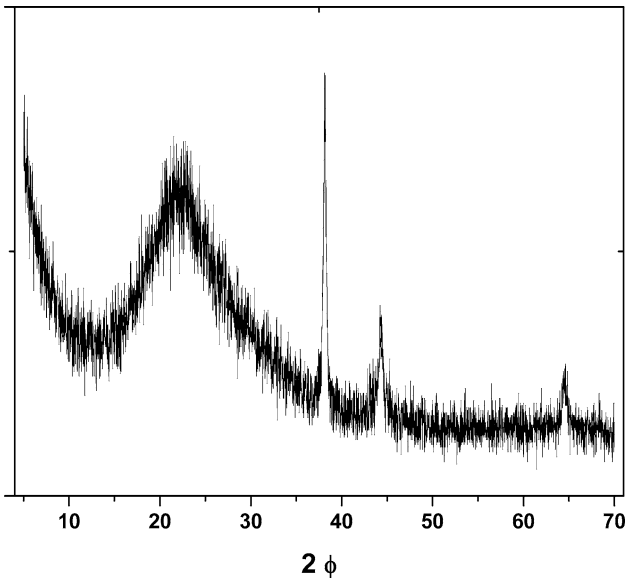

Fig. 7 XRD spectrum of colloidal silica with covalently bonded NP4 silver nanoparticles clusters

angle of the selected peak, and $B = (\beta^2 - \beta_0^2)^{1/2}$, where $\beta = 0.00613$ rad is the width at half height of the selected peak, and $\beta_0 = 0.00297$ rad is the width at half height of a reference peak (quartz). This gives $d = 28.6$ nm, a value that is close to the average value of 23 nm, calculated from TEM images.

This result indicates that Ag NPs are monocrystalline and do not undergo coalescence during the conditions used to produce the covalent bonding to the silica surface. However, it is expected that in addition to the covalent bonds formed with SiOH groups of the silica surface, Ag NPs should agglomerate as clusters by the formation of Si–O–Si bonds among the end groups of the stabilizing chains [20]. TEM images (Fig. 8) allow estimating the size of these clusters.

Table 1 Ag wt% for samples of SiO_2-NP

Sample	% Ag
SiO_2-NP2	0.510 ± 0.013
SiO_2-NP4	0.621 ± 0.041
SiO_2-NP8	0.860 ± 0.120

Figure 8 shows TEM images of (a) pure colloidal silica and (b) silica with covalently bonded NP4 Ag NPs. Large isolated silica particles are identified by a gray coloration. The overlapping of these particles generates a darker gray color in the images. Small black particles bonded to the surface of silica particles indicated by arrows are Ag NPs (they appear as black objects due to the high electronic density of silver).

Ag contents in the SiO_2-NP samples were determined by ICP and were found to be between 0.5 and 1 wt%. Results for the three samples are shown in Table 1.

Antibacterial properties of colloidal silica decorated with Ag NPs

Bacterial (*E. Coli*) growth was followed by measuring optical density (OD) at 600 nm for two control samples, a sample containing unmodified colloidal silica and samples containing different amounts of colloidal silica with NP4 Ag NPs (Fig. 9).

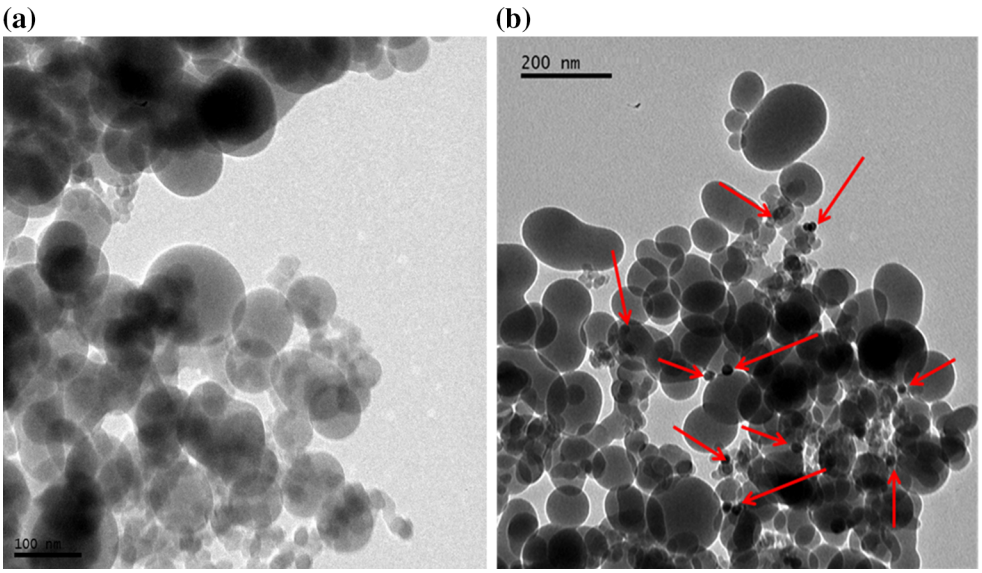

Fig. 8 TEM images of **a** pure colloidal silica and **b** silica with covalently bonded NP4 Ag NPs

Author's personal copy

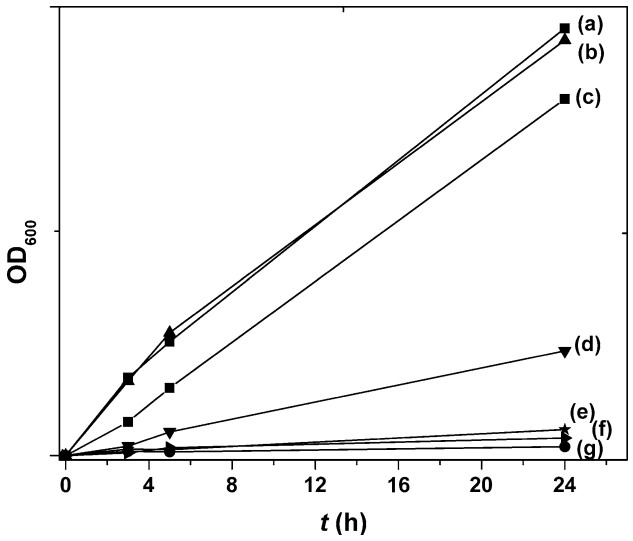

Fig. 9 OD_{600} versus growth time for different *E. Coli* cultures in LB medium: **a** control [+], **b** +1 wt% unmodified colloidal silica, **c** +0.2 wt% NP4-SiO_2, **d** +0.5 wt% NP4-SiO_2, **e** +1 wt% NP4-SiO_2, **f** +2 wt% NP4-SiO_2, **g** control [−]

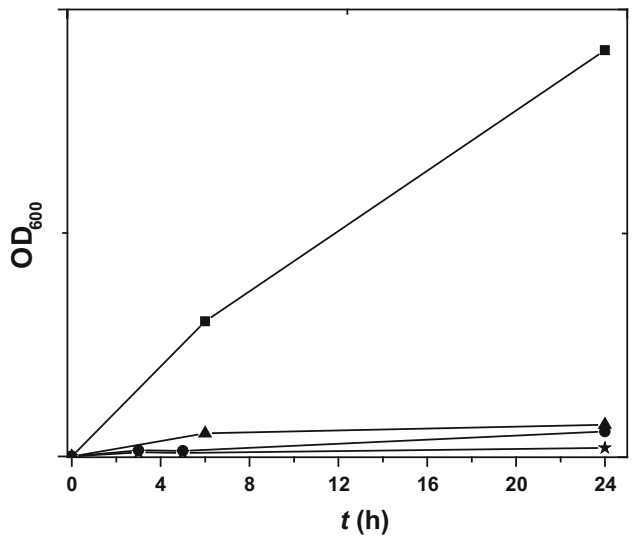

Fig. 10 OD_{600} versus growth time for different *E. Coli* cultures in LB medium: Control [+] (*square*), +1 wt% recycled NP4-SiO_2 (*triangle*), +1 wt% fresh NP4-SiO_2 (*circle*), Control [−] (*star*)

The curves for control [+] (without addition of extra materials) and for control [−] (with addition of an antibiotic) represent limiting cases of bacterial growth. Unmodified silica did not have any effect on bacterial growth, while the addition of colloidal silica decorated with Ag NPs produced a significant retard of this process, particularly for additions of 1 wt% or higher. Similar results were obtained with colloidal silica modified by NP2 and NP8 Ag NPs.

The sample containing 2 wt% NP4-SiO_2 was filtered after 24 h in contact with bacteria, and the solid was washed with ethanol–water 70:30 to kill any residual bacteria. Then, it was rinsed three times with water, dried at 110 °C for 2 h, and ground. Bactericidal properties of the recycled material were tested and shown to be practically the same as the one of the fresh product (Fig. 10).

The possibility of reusing the antibacterial powder might have practical applications. Besides, it provides an extra confirmation of the strong bonds generated between Ag NPs and colloidal silica.

Conclusions

Ag NPs were synthesized using glycerol as solvent and reducing agent and an aminotrialkoxysilane as a stabilizer. Broad size distributions were obtained with average sizes ranging from 13 to 55 nm, depending on the molar ratio of alkoxysilane/Ag used in the synthesis. Terminal alkoxysilanes reacted with OH groups of glycerol leading to the covalent bonding of glycerol moieties to the chain ends of the stabilizer. This produced extremely stable colloidal dispersions from which NPs could not be extracted with solvents immiscible with glycerol (as THF). Ag NPs were covalently bonded to the surface of a colloidal silica by hydrolysis/condensation of terminal Si–O–C bonds of the stabilizer with superficial SiOH bonds of silica. TEM images revealed the presence of individual NPs and small clusters of NPs attached to the silica surface. These clusters were presumably generated by intermolecular reactions among chain ends of the stabilizer producing Si–O–Si bonds. The colloidal silica decorated with Ag NPs had antibacterial properties and could be recycled after use.

Acknowledgement The financial support from the National Research Council (CONICET), the University of Mar del Plata and the National Agency for the Promotion of Science and Technology (ANPCyT), Argentina, is gratefully acknowledged. The authors wish to thank Giovani Pavoski and Prof. Griselda Barrera Galland for the ICP measurements at the UFRGS, Porto Alegre, Brazil.

Compliance with ethical standards

Conflict of interest The authors declare no competing financial interest.

References

1. Sondi I, Salopek-Sondi B (2004) Silver nanoparticles as antimicrobial agent: a case study on *E. coli* as a model for Gram-negative bacteria. J Colloid Interface Sci 275:177. doi:10.1016/j.jcis.2004.02.012
2. Rai M, Yadav A, Gade A (2009) Silver nanoparticles as a new generation of antimicrobials. Biotech Adv 27:76. doi:10.1016/j.biotechadv.2008.09.002
3. Rizzello L, Pompa PP (2014) Nanosilver-based antibacterial drugs and devices: mechanisms, methodological drawbacks, and guidelines. Chem Soc Rev 43:1501. doi:10.1039/c3cs60218d

Author's personal copy

4. Vukoje ID, Džunuzović ES, Vodnik VV, Dimitrijević S, Ahrenkiel SP, Nedeljković JM (2014) Synthesis, characterization, and antimicrobial activity of poly(GMA-co-EGDMA) polymer decorated with silver nanoparticles. J Mater Sci 49:6838–6844. doi:10.1007/s10853-014-8386-x
5. Zhang D, Toh GH, Lin H, Chen Y (2012) In situ synthesis of silver nanoparticles on silk fabric with PNP for antibacterial finishing. J Mater Sci 47:5721–5728. doi:10.1007/s10853-012-6462-7
6. Shinde VV, Jadhav PR, Kim JH, Patil PS (2013) One-step synthesis and characterization of anisotropic silver nanoparticles: application for enhanced antibacterial activity of natural fabric. J Mater Sci 48:8393–8401. doi:10.1007/s10583-013-7651-8
7. Ahamed M, Alsalhi MS, Siddiqui MK (2010) Silver nanoparticle applications and human health. Clinica Chim Acta 411:1841. doi:10.1016/j.cca.2010.08.016
8. Zhao CM, Wang WX (2010) Biokinetic uptake and efflux of silver nanoparticles in Daphnia magna. Environ Sci Technol 44:7699. doi:10.1021/es101484s
9. Frattini A, Pellegri N, Nicastro D, de Sanctis O (2005) Effect of amine groups in the synthesis of Ag nanoparticles using aminosilanes. Mater Chem Phys 94:148. doi:10.1016/j.matchemphys.2005.04.023
10. Nogueira AL, Machado RAF, de Souza AZ, Martinello F, Franco CV, Dutra GB (2014) Synthesis and characterization of silver nanoparticles produced with a bifunctional stabilizing agent. Ind Eng Chem Res 53:3426. doi:10.1021/ie4030903
11. Wu KH, Chang YC, Tsai WY, Huang MY, Yang CC (2010) Effect of amine groups on the synthesis and antibacterial performance of Ag nanoparticles dispersed in aminosilanes-modified silicate. Polym Degrad Stab 95:2328. doi:10.1016/j.polymdegradstab.2010.08.025
12. Wu KH, Liu CI, Yang CC, Wang GP, Chao CM (2011) Preparation and characterization of aminosilane-modified silicate supported with silver for antibacterial behavior. Mater Chem Phys 125:802. doi:10.1016/j.matchemphys.2010.09.055
13. Lv Y, Liu H, Wang Z, Liu S, Hao L, Sang Y, Liu D, Wang J, Boughton RI (2009) Silver nanoparticle-decorated porous ceramic composite for water treatment. J Membr Sci 331:50. doi:10.1016/j.memsci.2009.01.007
14. Fasce DP, Williams RJJ, Méchin F, Pascault JP, Llauro MF, Pétiaud R (1999) Synthesis and characterization of polyhedral silsesquioxanes bearing bulky functionalized substituents. Macromolecules 32:4757. doi:10.1021/ma981875p
15. Fasce DP, Williams RJJ, Erra-Balsells R, Ishikawa Y, Nonami H (2001) One-step synthesis of polyhedral silsesquioxanes bearing bulky substituents: UV-MALDI-TOF and ESI-TOF mass spectrometry characterization of reaction products. Macromolecules 34:3534. doi:10.1021/ma001711k
16. dell'Erba IE, Fasce DP, Williams RJJ, Erra-Balsells R, Fukuyama Y, Nonami H (2003) Poly(silsesquioxanes) derived from the hydrolytic condensation of organotrialkoxysilanes containing hydroxyl groups. J Organomet Chem 686:42. doi:10.1016/S0022-328X(03)00377-2
17. dell'Erba IE, Hoppe CE, Williams RJJ (2010) Synthesis of silver nanoparticles coated with OH-functionalized organic groups: dispersion and covalent bonding in epoxy networks. Langmuir 26:2042. doi:10.1021/la902568v
18. Patterson AL (1939) The Scherrer formula for X-ray particle size determination. Phys Rev 56:978. doi:10.1103/PhysRev.56.978
19. Langford JI, Wilson AJC (1978) Scherrer after sixty years: a survey and some new results in the determination of crystallite size. J Appl Cryst 11:102. doi:10.1107/S0021889878012844
20. dell'Erba IE, Hoppe CE, Williams RJJ (2012) Films of covalently bonded gold nanoparticles synthesized by a sol–gel process. J Nanopart Res 14:1098. doi:10.1007/s11051-012-1098-8